Leukemia
https://doi.org/10.1038/s41375-020-0764-6

ARTICLE

Acute myeloid leukemia

Simultaneous kinase inhibition with ibrutinib and BCL2 inhibition with venetoclax offers a therapeutic strategy for acute myeloid leukemia

Christopher A. Eide[1,2] · Stephen E. Kurtz[1] · Andy Kaempf[3] · Nicola Long[1] · Anupriya Agarwal[1] · Cristina E. Tognon[1,2] · Motomi Mori[3,4] · Brian J. Druker[1,2] · Bill H. Chang[1] · Alexey V. Danilov[1] · Jeffrey W. Tyner[1,5]

Received: 7 June 2019 / Revised: 7 February 2020 / Accepted: 12 February 2020

Abstract

Acute myeloid leukemia (AML) results from the enhanced proliferation and impaired differentiation of hematopoietic stem and progenitor cells. Using an ex vivo functional screening assay, we identified that the combination of the BTK inhibitor ibrutinib and BCL2 inhibitor venetoclax (IBR + VEN), currently in clinical trials for chronic lymphocytic leukemia (CLL), demonstrated enhanced efficacy on primary AML patient specimens, AML cell lines, and in a mouse xenograft model of AML. Expanded analyses among a large cohort of hematologic malignancies ($n = 651$ patients) revealed that IBR + VEN sensitivity associated with selected genetic and phenotypic features in both CLL and AML specimens. Among AML samples, 11q23 MLL rearrangements were highly sensitive to IBR + VEN. Analysis of differentially expressed genes with respect to IBR + VEN sensitivity indicated pathways preferentially enriched in patient samples with reduced ex vivo sensitivity, including IL-10 signaling. These findings suggest that IBR + VEN may represent an effective therapeutic option for patients with AML.

Introduction

The identification of effective therapies based on targeted interventions for human cancers faces the challenges of genetic and epigenetic heterogeneity underlying the disease. Large-scale sequencing efforts have uncovered a spectrum of mutations in many hematologic malignancies, suggesting that combinations of agents will be required to treat these diseases effectively. For patients with acute myeloid leukemia (AML), the long-standing frontline chemotherapy consisting of cytarabine and anthracyclines has a 5-year overall survival rate of 25% [1]. Outcomes in older patients, who represent the majority of patients with this disease, are poor with a median survival of 5–10 months. Due to their inability to tolerate intensive chemotherapy, many older patients do not receive any antileukemic therapy [2].

Although molecularly targeted drugs offer substantial promise as treatment options, the effectiveness of individual inhibitors has been limited by resistance mutations and activation of compensatory signaling pathways. Resistance to targeted agents in AML is further complicated by substantial disease heterogeneity and rescue signals from the microenvironment, underscoring the need for combinations of targeted therapies to achieve durable responses.

Recent reports demonstrating the efficacy of combinations of oral, targeted drugs for several adult leukemias establish their potential for improved and durable clinical

These authors contributed equally: Christopher A. Eide, Stephen E. Kurtz

Supplementary information The online version of this article (https://doi.org/10.1038/s41375-020-0764-6) contains supplementary material, which is available to authorized users.

✉ Jeffrey W. Tyner
tynerj@ohsu.edu

[1] Division of Hematology & Medical Oncology, Knight Cancer Institute, Oregon Health & Science University, Portland, OR, USA

[2] Howard Hughes Medical Institute, Portland, OR, USA

[3] Biostatistics Shared Resource, Knight Cancer Institute, Oregon Health & Science University, Portland, OR, USA

[4] Portland State University and Oregon Health & Science University School of Public Health, Portland, OR, USA

[5] Department of Cell, Developmental, and Cancer Biology, Oregon Health & Science University, Portland, OR, USA

Published online: 24 February 2020

responses, and shift treatment options away from cytotoxic chemotherapy. The BCL2 inhibitor, venetoclax, has demonstrated single-agent efficacy in patients with AML [3], and the combination of venetoclax plus a hypomethylating agent was recently approved as a therapeutic strategy for elderly, treatment-naive AML patients [4, 5]. However, responses are of short duration, justifying exploration of additional therapeutic strategies. For chronic lymphocytic leukemia (CLL) and mantle cell lymphoma (MCL), combinations of the BTK inhibitor ibrutinib with the BCL2 inhibitor venetoclax have shown dramatic response in patients with high rates of minimal residual disease negativity [6–9]. Both ibrutinib and venetoclax as single agents are highly effective in CLL, though their primary mechanisms of action are different; while both drugs induce direct killing, ibrutinib also induces CLL cell egress from the nurturing lymph node microenvironment resulting in redistribution into the peripheral blood [10]. Tumor cells isolated from patients receiving ibrutinib for MCL also show venetoclax sensitivity [11]. Notably, the effectiveness of this combination is anticipated from prior studies showing that tumor cells isolated from CLL patients on ibrutinib monotherapy are highly sensitive to venetoclax [12, 13].

Efforts to identify new targeted combinations for AML have been aided by the use of ex vivo functional screening of primary patient leukemia cells [14]. Using this approach, the recent publication of functional and genomic data for a large cohort of AML patient samples described a significant association between samples with *FLT3-ITD*, *NPM1*, and *DNMT3A* mutations and sensitivity to ibrutinib [15]. This observation prompted us to test the combination of ibrutinib with venetoclax on AML patient samples, given the emerging success of this combination in CLL.

Methods

Patient samples

All patients gave informed consent to participate in this study, which had the approval and guidance of the Institutional Review Boards at Oregon Health & Science University (OHSU), University of Utah, University of Texas Medical Center Southwestern, Stanford University, University of Miami, University of Colorado, University of Florida, National Institutes of Health, Fox Chase Cancer Center, and University of Kansas. Samples were sent to the coordinating center (OHSU IRB 9570 and 4422), where they were coded and processed. Primary bone marrow aspirates or peripheral blood draws from 651 unique patients with hematologic malignancies were collected and classified according to five general diagnostic groups: AML ($n = 325$), CLL ($n = 152$), acute lymphoblastic leukemia (ALL; $n = 100$), chronic myeloid leukemia (CML; $n = 27$), and myeloproliferative neoplasms or myelodysplastic syndromes (MPN or MDS/MPN; $n = 47$). Samples were assayed for drug sensitivity within 24 h of receipt. All samples were analyzed for clinical characteristics, with expanded, disease-specific panels of clinical, prognostic, genetic, cytogenetic, and surface antigen characteristics obtained from AML and CLL patient's electronic medical records. Genetic characterization of AML samples included results of a clinical deep-sequencing panel of genes commonly mutated in hematologic malignancies.

Cell lines

Human AML patient-derived MOLM14 (FLT3-ITD positive), HL60, and GDM1 cells were obtained from DSMZ and maintained in RPMI1640 media supplemented with 10% fetal bovine serum (FBS), 100 U/mL penicillin/100 µg/mL streptomycin, and 2 mmol/L L-glutamine (R10) at 37 °C in 5% CO_2. Cells were kept in culture no longer than a month at a time, and all cell lines were authenticated by extensive functional and genetic analysis in our lab.

Ex vivo functional screen

Small-molecule inhibitors, purchased from LC Laboratories (Woburn, MA, USA) and Selleck Chemicals (Houston, TX, USA), were reconstituted in DMSO and stored at −80 °C. Inhibitors were distributed into 384-well plates prepared with single agents in a seven-point concentration series (10–0.0137 µM) and the combination of ibrutinib and venetoclax in a seven-point equimolar ratio concentration series identical to those used for single agents. The final concentration of DMSO was ≤0.1% in all wells, and all plates were stored at −20 °C and thawed immediately prior to use. Primary mononuclear cells freshly isolated by Ficoll-gradient centrifugation were seeded into 384-well assay plates at 10,000 cells/well in RPMI1640 media supplemented with FBS (10%), L-glutamine, penicillin-streptomycin, and b-mercaptoethanol (10^{-4} M). After 3 days of culture at 37 °C in 5% CO_2, methanethiosulfonate reagent (CellTiter 96 AQ_{ueous} One; Promega Madison, WI, USA) was added to each well and absorbance was measured at 490 nm.

Inhibitor dose–response curve analysis and effect-measure calculations

Raw absorbance values were adjusted to a reference blank value (average of positive-control wells containing a drug combination of flavopiridol, staurosporine, and velcade), normalized to untreated control wells, and bounded at 0 and

100 to produce cell viability percentages. Normalized viability percentages [16] at each dose of single agent or combination of seven-point dilution series were analyzed for all patient samples that passed a quality control inspection (based on plate- and profile-specific expectations of drug-induced cell inhibition). A two-parameter probit regression curve was fit to each seven-point $\log_{10}$-transformed dose–response profile using maximum likelihood estimation for the intercept and slope. This parametric model was chosen over a polynomial because the probit's monotonic shape reflects a dose–response curve typically seen in samples incubated with cytotoxic or inhibitory agents [17]. From the fitted probit curve for each sample-drug pairing, the half maximum inhibitory concentration (IC_{50}) was defined as the lowest concentration to achieve 50% predicted viability, and the area under the curve (AUC) was computed by the integration of the curve height across the tested dose range. If the predicted cell viability (i.e., probit curve height) was ≤50% at the lowest tested dose or >50% across the entire dose range, the IC_{50} was designated as the lowest dose or highest dose, respectively. For sensitivity profiles with 100% normalized viability at all seven dose points, the IC_{50} and AUC were designated as the highest tested dose and the maximum possible AUC, respectively. For sensitivity profiles with 0% viability at all seven dose points, the IC_{50} and AUC were designated as the lowest tested dose and a value (0.01) just below the minimum probit-derived AUC, respectively.

Mouse xenograft model

NSG mice were purchased from JAX Labs as 5 weeks old, females, and allowed to acclimate for 1 week prior to the study. MOLM13 cells were injected into tail veins of NSG mice (3×10^5 cells/mouse) and allowed to engraft for 48 h. Thereafter, mice (5 per group) were treated daily by oral gavage with vehicle, venetoclax (25 mg/kg), ibrutinib (25 mg/kg), or the IBR + VEN combination administered sequentially; i.e., venetoclax (25 mg/kg) followed 2 h later with ibrutinib (25 mg/kg). On day 17 (15 days of treatment), animals were euthanized and assessed for disease burden. This study was approved by the OHSU IACUC.

Gene expression and pathway enrichment analysis

A differential expression (DE) analysis pipeline was applied to AML patient specimens with ex vivo IBR + VEN sensitivity data and RNA sequencing data available (collected under the Beat AML study [15]). Genes were removed for having >1 HGNC symbol or read counts <10 in at least 90% of samples. Specimens whose median expression value (across all nonfiltered genes) was <2 standard deviations below the mean (for this AML sample set) were removed from consideration, and the earliest specimen was chosen for patients with multiples. Next, "sensitive" and "resistant" sample groups were identified as the lowest 25% and highest 25%, respectively, of specimens according to combination drug AUC. To account for differences in library size, GC content, and gene length, conditional quantile normalization [18] was applied to the remaining gene-by-sample matrix of read counts to generate (1) $\log_2$ normalized RPKM values for correlation analysis and visual clustering and (2) normalization factors for DE analysis using the DESeq2 method [19]. Latent variables representing potential batch effects were identified by count-based surrogate variable analysis [20, 21] and entered as covariates into the DESeq2 model to produce gene expression fold changes (resistant group/sensitive group) and associated Wald test false discovery rate (FDR)-adjusted p values [22]. Genes with adjusted p values < 0.01 were considered DE. For pathway topology analysis, reaction-based Reactome pathways [23, 24] were converted to gene/protein networks using the "graphite" R/Bioconductor package [25] and, after mapping DESeq2 $\log_2$ fold changes from Ensembl IDs to Uniprot IDs, tested for significant enrichment of DE gene products using the Pathway Regulation Score (PRS) method [26]. The PRS algorithm, as implemented by the "ToPASeq" R package [27], returns normalized (by pathway size) enrichment scores and FDR-adjusted p values calculated from null distributions generated by repeatedly permuting the gene labels on the list of fold changes.

IGHV mutation status

Following RNA and cDNA isolation, *IGHV* mutations were analyzed using the IGH Somatic Hypermutation Assay v2.0 (Invivoscribe). Briefly, PCR was performed using the supplied master mixes and Amplitaq Gold DNA polymerase (Applied Biosystems) on a Veriti Thermal Cycler Model #9902 (Applied Biosystems) to amplify the *IGH* sequence fragment between the leader (VHL) and joining (J) regions as per the manufacturer's instructions. To confirm the amplification of a single clonal product in the expected size range, an aliquot of each sample was run on a 1.5% agarose gel and separated by gel electrophoresis. Samples were then submitted for DNA sequencing using the supplied sequencing primers. The NCBI IgBLAST tool was used to determine the % divergence of each clonal sequence. Samples which showed <2% divergence from germline sequence were deemed to have unmutated *IGHV*.

Assessment of plasma cytokine levels

Plasma isolated and banked from patient samples at the time of ex vivo assay evaluation was assayed for a panel of human

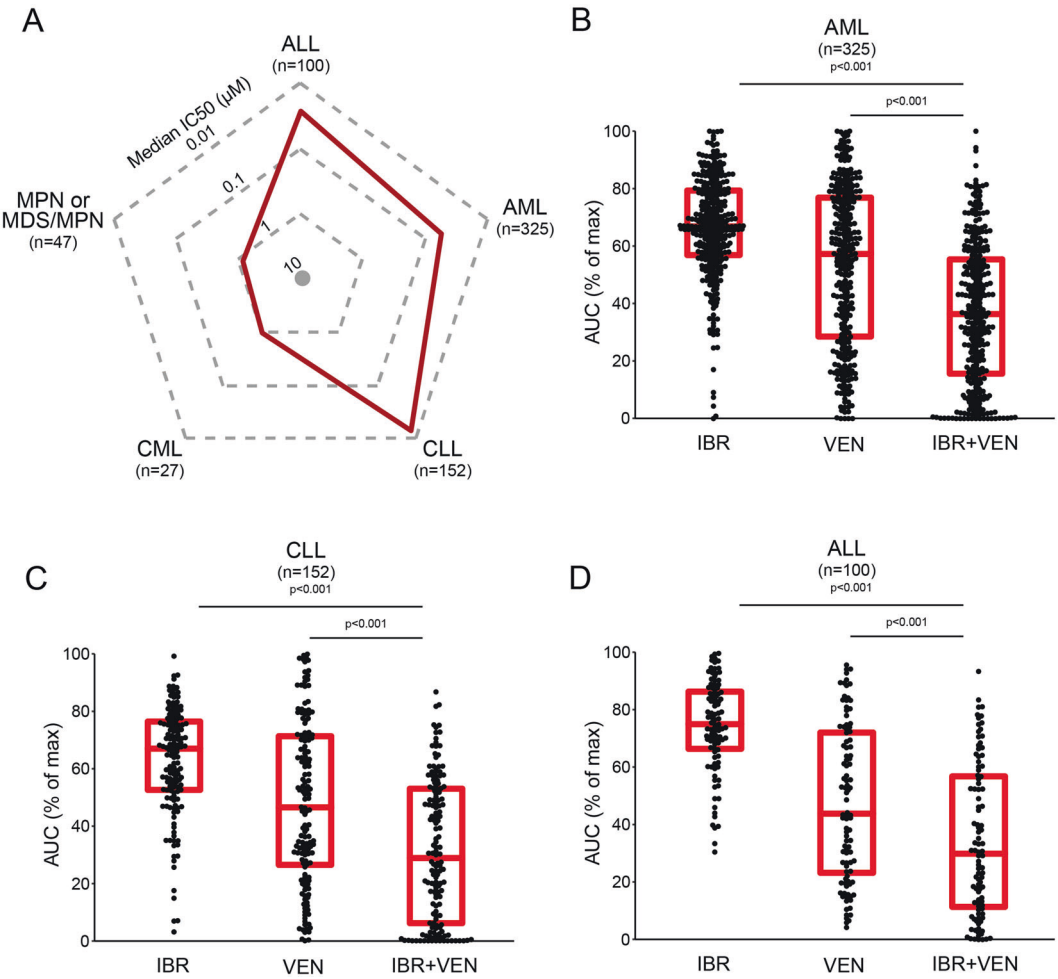

Fig. 1 Sensitivity of Ibrutinib + Venetoclax combination on 651 unique leukemia patient samples. a Radar plot indicating median IC_{50} values (red line) for 651 unique patient samples across five leukemia subgroups. **b–d** Comparisons of ibrutinib (IBR) and venetoclax (VEN) sensitivities alone and in combination for AML, CLL, and ALL subgroups. Red horizontal bars indicate median and interquartile range for % of maximum AUC. Comparisons were performed with Nemenyi test for the combination to each single agent.

inflammatory cytokines using the Luminex platform (R&D Systems) according to the manufacturer's protocol. Cytokine values were normalized to total protein levels for each sample.

Statistical analysis

IBR + VEN efficacy was compared for all samples ($n = 651$) across a panel of general clinical and disease-specific variables. Subgroups for all mutations, cytogenetic abnormalities, and cell surface antigens were defined as either positive or negative. Combination sensitivity (as measured by % of maximum AUC) for categorical variables was compared using a Mann–Whitney or Kruskal–Wallis test. Comparisons of matched single agent and combination treatment sensitivity were performed using Friedman test with Dunn's post-hoc pairwise comparisons. Correlations between continuous clinical variables (e.g., WBC count) and drug sensitivity values were evaluated with Spearman's rank correlation coefficients. In vivo response data were compared between treatment groups using a one-way ANOVA test with Hochberg's step-up Bonferroni adjustment of p values for pairwise group comparisons [28]. Plasma cytokine data were compared between IBR + VEN sensitive and resistant samples using a Mann–Whitney test.

Results

AML cells are highly sensitive to ibrutinib combined with venetoclax (IBR + VEN)

Ex vivo screening of primary cells from patients with various hematologic malignancies (Supplementary File S1) including AML ($n = 325$), CLL ($n = 152$), ALL ($n = 100$), MPN or MDS/MPN ($n = 47$), and CML ($n = 27$) revealed several interesting patterns of sensitivity. Sensitivities to the IBR + VEN combination are represented in the radar plot depicting IC_{50} values across the five diagnostic groups (Fig. 1a). Consistent with clinical data and previous

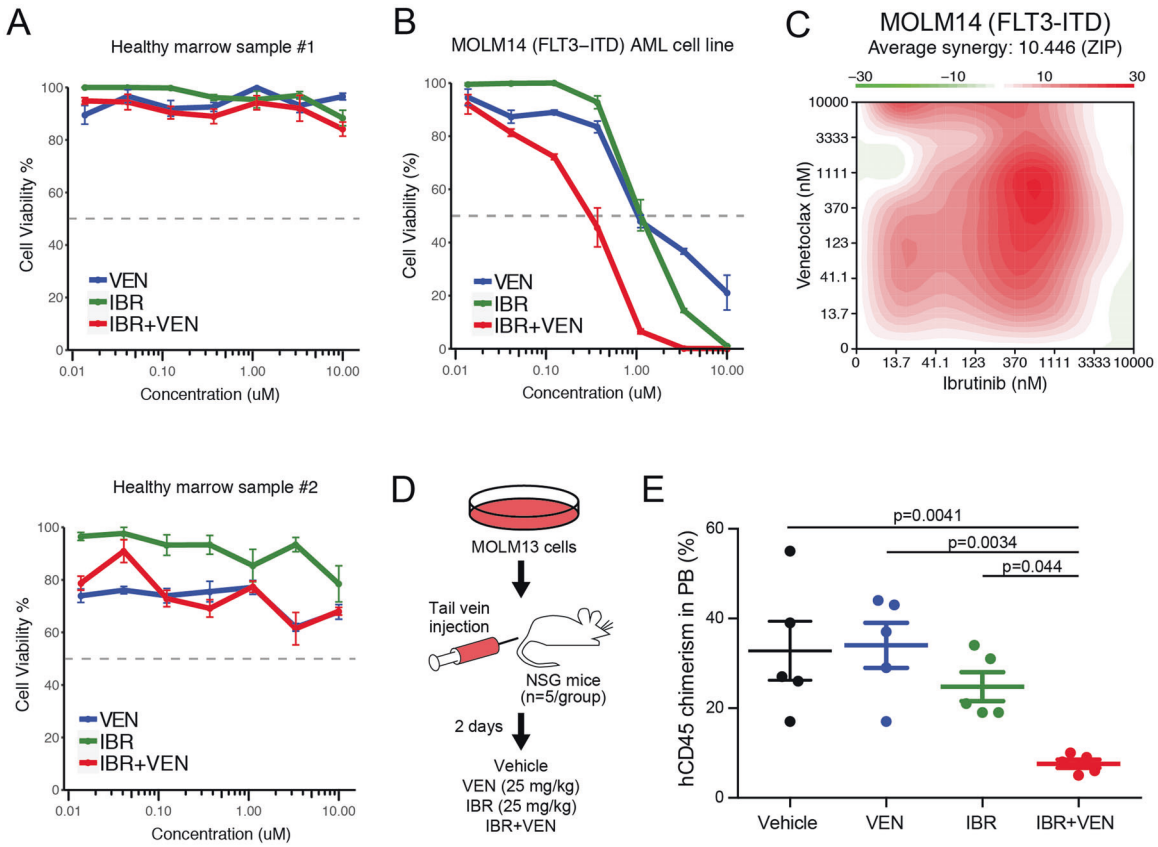

Fig. 2 Ibrutinib + Venetoclax combination is potent and synergistic in AML cells. a Evaluation of IBR and VEN alone and in combination on two healthy donor bone marrow samples. **b** Evaluation of IBR and VEN alone and in combination on MOLM14 AML cells. **c** Surface plot of IBR + VEN synergy (ZIP score) generated from a 7 × 7 dose matrix on MOLM14 AML cells. Synergy was calculated with the R package "synergyfinder" [51]. **d** Schematic of in vivo xenograft study. **e** Levels of human CD45-positive cells in peripheral blood of NSG mice injected with MOLM13 cells and treated with vehicle, venetoclax (25 mg/kg), ibrutinib (25 mg/kg), or the combination IBR + VEN (25 mg/kg each). Hochberg-adjusted *p* values are indicated for comparisons with the combination.

literature, the IBR + VEN combination was highly effective in CLL specimens (median $IC_{50} = 0.015$ μM). Intriguingly, IBR + VEN also showed similar effectiveness on ALL and AML primary samples (median IC_{50}: 0.018 and 0.054 μM, respectively). By contrast, samples from patients with CML or MDS/MPN were markedly less sensitive to the combination, with median IC_{50} values near or above 1 μM.

Among the three sensitive diagnostic subgroups, in each case the IBR + VEN combination demonstrated superior efficacy compared with either single agent by two different effect measures (IC_{50} and AUC; Fig. 1b–d). For example, IBR + VEN was 20- to 80-fold more potent by IC_{50} across AML patient specimens compared with venetoclax and ibrutinib alone, respectively (adjusted $p < 0.001$).

We also tested this combination on primary cells from two healthy donors to evaluate potential broader toxicity. In contrast to our findings with AML patient specimens, healthy donor mononuclear cells showed little to no sensitivity to IBR + VEN (Fig. 2a). To validate our AML findings and to establish whether the efficacy of the IBR + VEN combination represents a synergistic relationship, the combination was tested for sensitivity on the human AML cell lines MOLM14, HL60, and GDM1 using a dose matrix, which included all possible concentration pairings for each drug's seven-point dose series. MOLM14 cells were modestly sensitive to both ibrutinib and venetoclax as single agents, but demonstrated enhanced efficacy when used in combination (Fig. 2b and Supplementary Fig. S1). Synergy scores were calculated using the zero interaction potency (ZIP) model for each dose pair of the 7 × 7 matrix; a positive score indicates synergy relative to the expected cell inhibition when assuming no interaction [29]. By this method, the IBR + VEN combination showed synergy in MOLM14, HL60, and GDM1 cells across the surveyed dose matrix (average ZIP score: +10.4, +3.5, and +20.1, respectively; Fig. 2c and Supplementary Fig. S1).

The IBR + VEN combination was also found to be effective in vivo, where it reduced tumor burden relative to either single agent as assessed by a decrease in human CD45-positive cells in peripheral blood of NSG mice injected with MOLM13 cells (Fig. 2d, e). IBR + VEN also reduced spleen weight relative to either single agent,

whereas neither hemoglobin levels nor platelet counts were altered across the treatment groups (Supplementary Fig. S2). Together, these findings suggest that IBR + VEN is well tolerated and demonstrates enhanced efficacy in an in vivo AML xenograft model.

Genetic and clinical features associate with differential sensitivity to IBR + VEN ex vivo

To identify associations between relevant patient characteristics and combination sensitivity ex vivo, IBR + VEN efficacy (as measured by AUC) was broken down according to general clinical and disease-specific features for CLL and AML, our two largest diagnosis categories. For CLL samples, del(11q) was associated with increased sensitivity to IBR + VEN ($p = 0.008$), whereas samples with mutated *IGHV* had reduced sensitivity ($p = 0.040$) (Fig. 3a). In addition, higher counts for WBCs and lymphocytes were correlated with increased sensitivity to the combination (Spearman's r: −0.39 and −0.45, respectively; $p < 0.001$). Conversely, and consistent with the latter, samples with higher percentages of monocytes were less sensitive (Spearman's r: 0.35; $p < 0.001$) (Fig. 3b).

Our AML cohort ($n = 325$) included patients with a wide range of disease subtypes representing both newly diagnosed and relapsed/refractory status. Among AML specimens, increased sensitivity to the combination of IBR + VEN was significantly associated with MLL rearrangement (t(v;11)(v;q23); $p = 0.035$), PML–RARA translocation (t(15;17); $p = 0.019$), *FLT3-ITD* ($p < 0.001$), and *NPM1* mutations ($p < 0.001$) (Fig. 4a). Other clinical/genetic features including inv(16), prior MDS, loss of chromosome 7, and RUNX1–RUNXT1 (t(8;21)) translocations were associated with reduced sensitivity to the combination (range of p values: <0.001–0.026). Moreover, higher percentages of bone marrow and peripheral blasts were correlated with increased sensitivity to the combination (Spearman's r: −0.39 and −0.37, respectively; $p < 0.001$) (Fig. 4b); a similar trend has been reported for venetoclax as a single agent [30].

IBR + VEN sensitivity relative to the expression of their respective canonical targets

Expression levels (normalized RPKM) of *BTK* and *BCL2*, the respective canonical targets of ibrutinib and venetoclax, were compared with sensitivity to the combination for a subset of the AML cohort (56%; 181/325) with available RNA-seq data (Fig. 4c). Higher expression levels of *BCL2* correlated with sensitivity to the combination as evaluated by AUC (Spearman's $r = -0.46$; $p < 0.001$), whereas expression levels of *BTK* were not significantly correlated with sensitivity to the combination (Spearman's $r = -0.10$; $p = 0.191$).

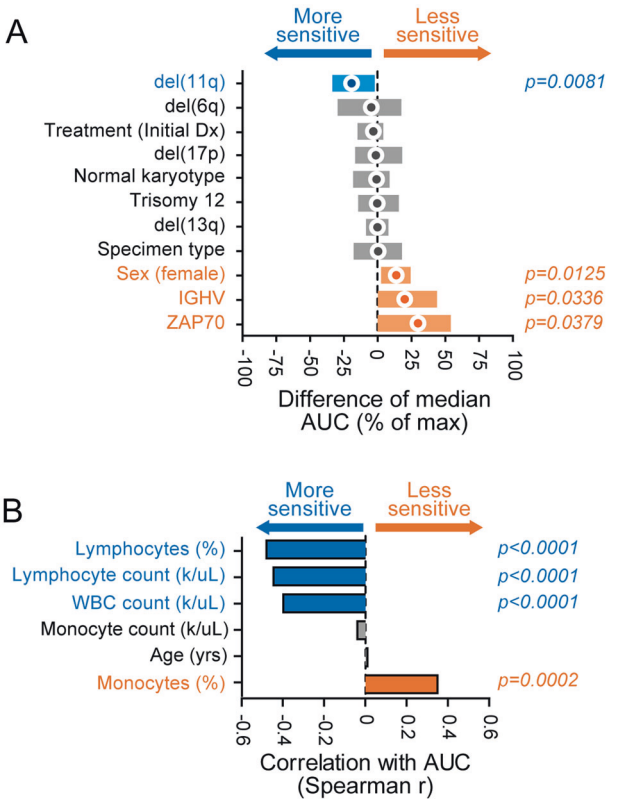

Fig. 3 Select clinical and genetic features in CLL samples associate with differential sensitivity ex vivo to Ibrutinib + Venetoclax. Comparisons of IBR + VEN sensitivities (% of max AUC) with respect to categorical variables (**a**) and continuous variables (**b**). Categorical variables were compared by Mann–Whitney test; circles indicate difference of median AUC and bars indicate 95% confidence interval. Continuous variables were correlated by Spearman's rank test.

Distinct patterns of differentially expressed genes associate with IBR + VEN sensitivity

DE analysis of the 25% most sensitive (AUC (% of max) ≤18.5; $n = 45$) vs. the 25% most resistant (AUC (% of max) >55.5; $n = 45$) AML samples to IBR + VEN yielded 7769 genes with an FDR-adjusted p value < 0.01 (DESeq2 method; Supplementary File S2). Unsupervised hierarchical clustering of the top 1000 most differentially expressed genes revealed marked differences between sensitive and resistant samples (Fig. 5a). Analysis across these two sample sets indicated higher *BCL2* expression levels associated with the IBR + VEN sensitive samples (FDR-adjusted $p = 1.18E{-}10$). Within the BCL2 family we and others [30, 31] observed higher levels of *BCL2A1* associated with IBR + VEN resistant samples (FDR-adjusted $p = 2.55E{-}16$) (Fig. 5b). Consistent with a lack of correlation between *BTK* expression levels and IBR + VEN sensitivity (Fig. 4c), *BTK* was not differentially expressed between IBR + VEN sensitive and resistant samples. However,

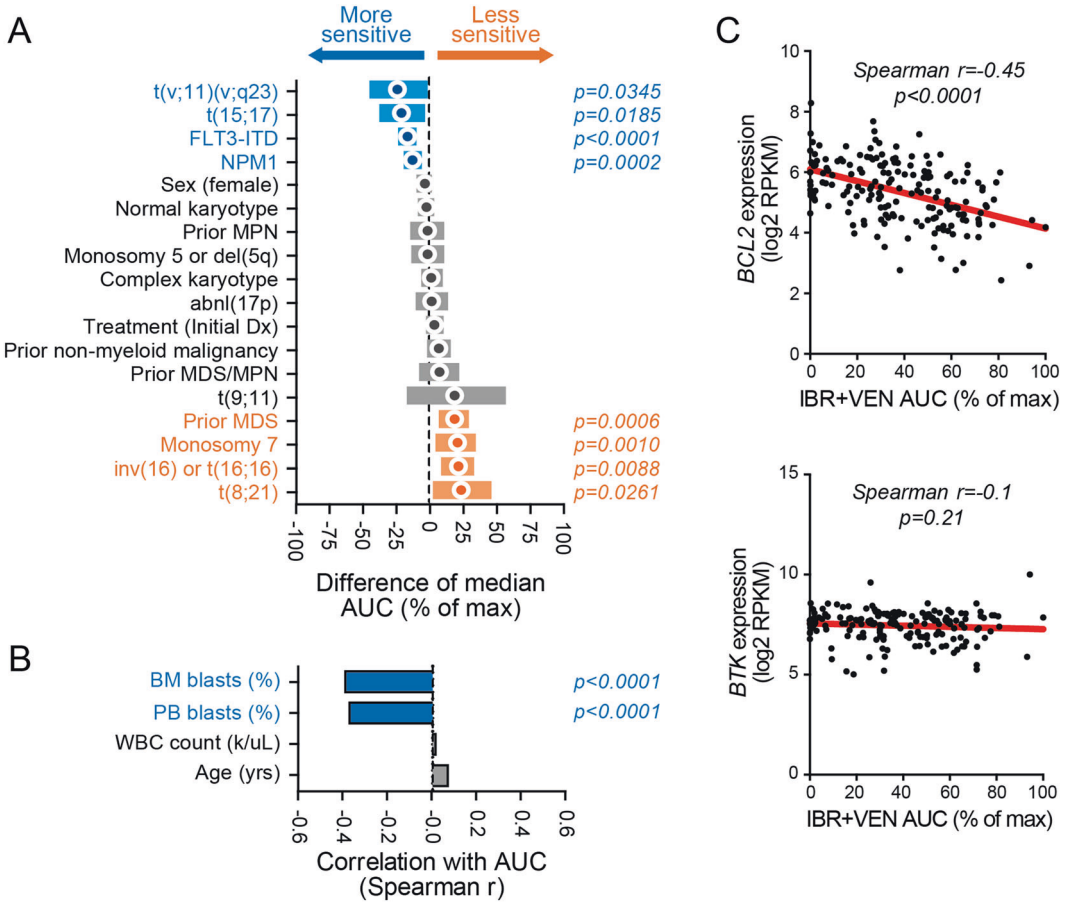

Fig. 4 Genetic abnormalities in AML samples associate with differential sensitivity ex vivo to Ibrutinib + Venetoclax. Comparisons of IBR + VEN sensitivities (% of max AUC) with respect to categorical variables (**a**) and continuous variables (**b**). Categorical variables were compared by Mann–Whitney test; circles indicate difference of median AUC and bars indicate 95% confidence interval. Continuous variables were correlated by Spearman's rank test. **c** Scatter plots of IBR + VEN AUC with expression levels of their respective canonical drug target: BTK and BCL2.

among other reported kinase targets of ibrutinib featuring the conserved cysteine aligning with C481 in BTK [32], two other TEC family members (TEC, TXK; Fig. 5b) and two ERBB family kinases (EGFR, ERBB2; Supplementary Fig. S3) showed significantly elevated expression levels in IBR + VEN sensitive samples (FDR-adjusted p value range: 2.56E−4 to 2.67E−7).

IL-10 signaling pathway genes are overexpressed in samples with ex vivo resistance to IBR + VEN

The fold changes of differentially expressed genes (defined as genes with FDR-adjusted $p < 0.01$) and the functional connections between their protein products in annotated biological pathways were combined via the PRS method [26] to identify significantly enriched Reactome pathways (Supplementary File S3). The IL-10 signaling pathway had one of the top enrichment scores, with 28 DE genes among the 39 genes belonging to this pathway. All but 2 of these 28 DE genes were upregulated in IBR + VEN resistant samples (Fig. 6a), suggesting that IL-10-dependent inflammatory cytokine pathways may contribute to decreased sensitivity to IBR + VEN. Notably, IL-10 dependent, NF-kB-mediated resistance mechanisms have been previously identified in MCLs for the IBR + VEN combination [33]. Concordantly, we detected elevated expression of *IL-10*, *CD40LG*, *NFKB1/2*, and *BIRC5* in IBR + VEN resistant patient samples (FDR-adjusted $p < 0.001$; Fig. 6b and Supplementary File S2).

We also evaluated the levels of inflammatory cytokines in plasma from a subset of the most and least IBR + VEN sensitive samples in our AML cohort. We observed increased levels of the pro-inflammatory cytokines TNF alpha and IFN gamma in IBR + VEN-resistant samples compared with sensitive samples (Supplementary Fig. S4). Correspondingly, RNA-seq-based expression levels of both of these genes were significantly increased in the resistant samples.

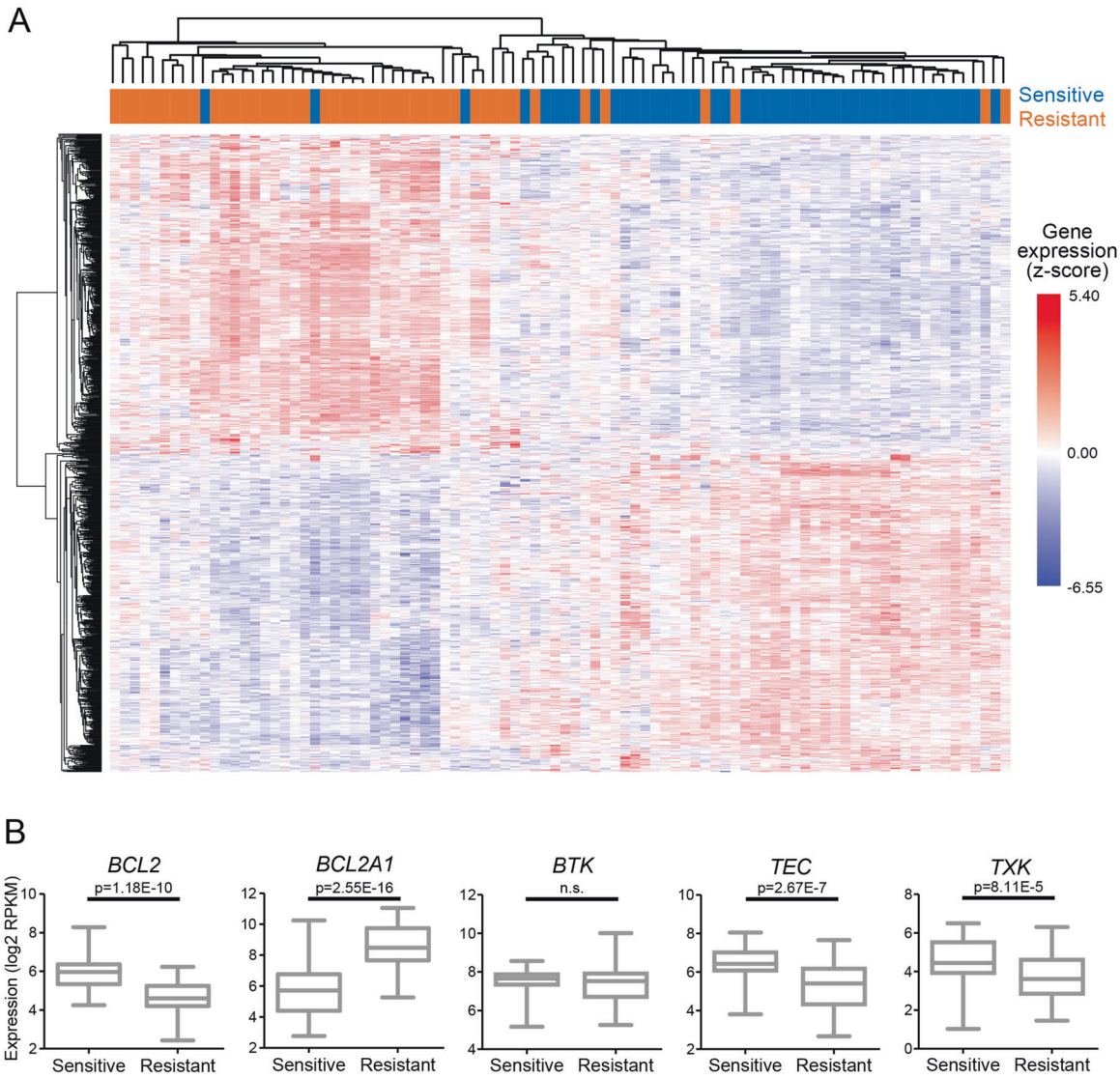

Fig. 5 Patterns of differentially expressed genes associate with sensitivity or resistance to IBR + VEN. a Hierarchical clustering of top 1000 DE genes between sensitive and resistant AML samples (lowest and highest quartile, respectively) by % of max AUC for IBR + VEN. Sensitive and resistant samples are designated in blue and orange, respectively, and expression values are represented as *z*-score. **b** Box plot comparisons of expression for select DE genes.

Discussion

The combination of IBR + VEN was previously identified as a promising therapeutic strategy for CLL and MCL [33–35]. These observations have prompted numerous clinical trials in which the combination has shown significant efficacy. Results presented from the CLARITY trial showed after 12 months on IBR + VEN combination treatment an absence of morphological evidence of CLL in the marrow biopsy and achievement of MRD-negative remission in 87% and 41% of patients, respectively [6]. Similarly high response rates were observed in the CAPTIVATE trial in cohorts of CLL patients with either relapsed/refractory or untreated high-risk disease [7, 9]. These promising outcomes, coupled with confirmation that the two drugs can be given in combination without obvious additional toxicity, are likely to alter the landscape of CLL therapy.

Our ex vivo drug testing process surveys patient samples across the full spectrum of hematologic malignancies, where we expectedly detected potent IBR + VEN sensitivity in primary CLL samples. Unexpectedly, our data revealed that the therapeutic potential of IBR + VEN may extend to AML, as demonstrated by the impressive sensitivity to this combination in our large patient sample set (median IC_{50}: 0.054 μM, $n = 325$). The IBR + VEN combination was more effective than either single agent at reducing tumor burden in vivo in a xenograft model of AML. Previously reported levels of each drug in plasma

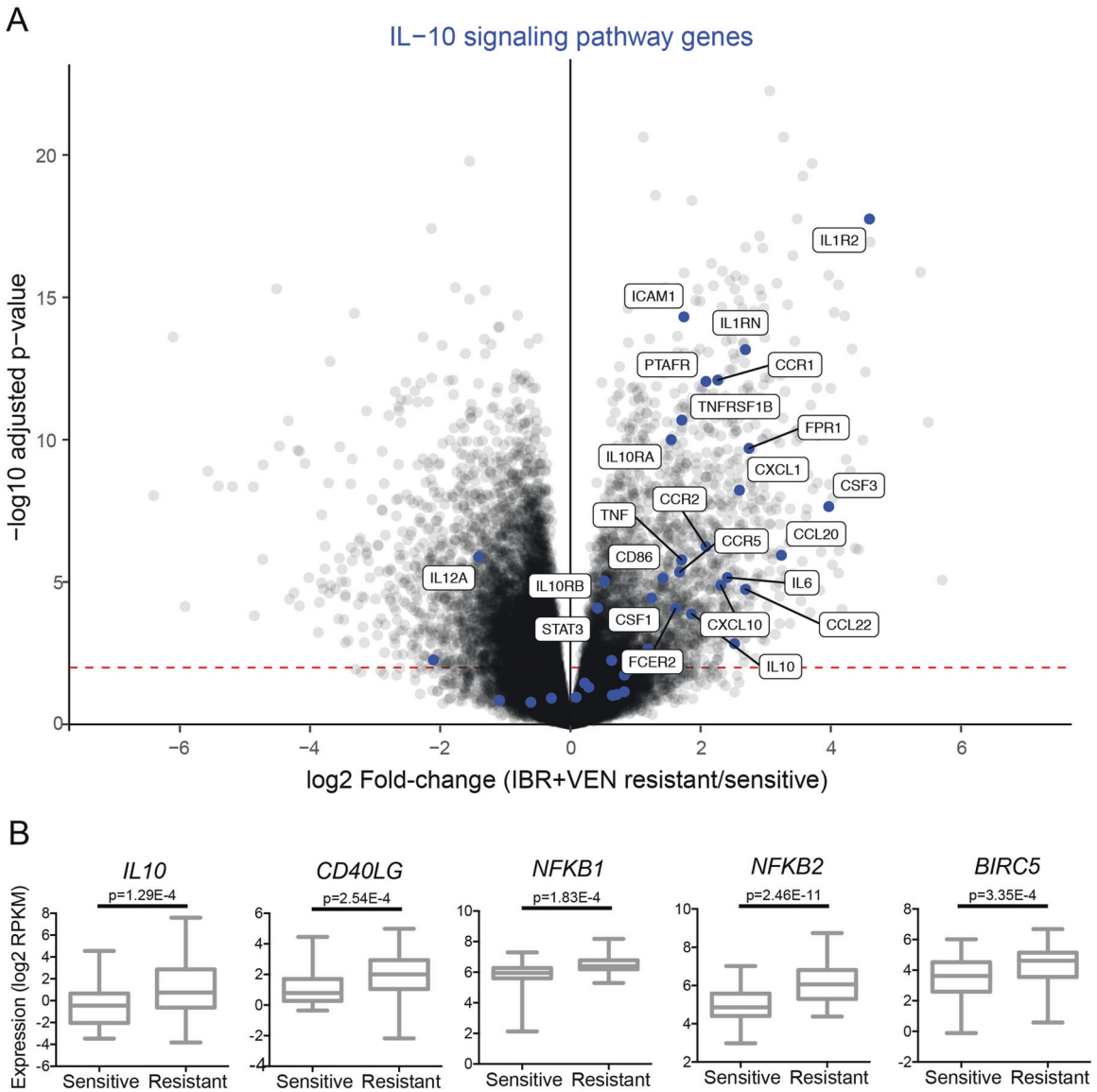

Fig. 6 Pathway analysis indicates that IL-10 signaling is enriched in IBR + VEN resistant samples. a The IL-10 signaling pathway is enriched in IBR + VEN resistant samples as represented in the volcano plot depicting the relative expression of ~22,000 genes. Genes involved in the IL-10 signaling pathway are highlighted by blue dots; differentially expressed genes with an adjusted p value < 0.001 are labeled. Red dashed line indicates p value of 0.01. **b** Dot plot comparisons of expression for select DE inflammatory signaling pathway genes.

(ibrutinib C_{max} for 140 mg QD: 0.084 μM [36]; venetoclax C_{max} for 400 mg QD: 2.51 μM [37]) suggest that effective combination concentrations would be achievable in patients. The most recent approval for AML has been for the use of venetoclax in combination with hypomethylating agents in newly diagnosed elderly patients not fit for standard chemotherapy [38]. In this setting, the initial response rates of 60–80% are highly encouraging; however, 1-year survival rates of 30–40% along with significantly lower activity in relapsed/refractory patients indicate that alternative venetoclax combinations may be beneficial.

Different clinical and genetic features of AML guide the selection of treatment options and/or confer altered risk stratification and prognosis. The most extreme example is that of the PML–RARA rearrangement (t(15;17)), which has an excellent prognosis when treated with the combination of arsenic trioxide and retinoic acid regimen [39]. By contrast, complex karyotype, monosomy 7/del(7q), monosomy 5/del (5q), TP53 mutations, and del(17p) are features of adverse risk patients with more limited treatment options. Among the panel of clinical and genetic features of AML for which we had available annotations, we found select features showing

either increased (11q23 MLL and PML–RARA rearrangements, FLT3-ITD and NPM1 mutations) or decreased (inv (16), monosomy 7, RUNX1–RUNXT1 rearrangement, prior MDS) sensitivity to this combination. Importantly, there were no significant differences in sensitivity to IBR + VEN observed for several features typically associated with adverse risk, including complex karyotype, abnormal 17p, prior MPN, and deletion of chr5 or 5q. With respect to CLL patient samples, the characteristics most associated with increased sensitivity to IBR + VEN were del(11q), male gender, and non-mutated *IGHV*. Our clinical record mining for mutated genes in CLL patients was restricted to *IGHV*, as this gene has prognostic impact for treatment. It is formally possible that unsurveyed genes or mutations may contribute to lower sensitivity to the combination.

Combined inhibition of BTK and BCL2, the respective canonical targets of ibrutinib and venetoclax, represents a possible mechanism of IBR + VEN efficacy. BTK has been shown to contribute to proliferation, survival, and migration in AML blast cells [40, 41], and it is possible that ibrutinib acts predominately on this kinase. It is also possible that the sensitivity of AML specimens to IBR + VEN represents an "overlapping" leukemia [42], although such biphenotypic leukemias are uncommon among adults (<1% of all acute leukemias) and the median age among AML patient samples in our cohort was 60.9 years. Furthermore, a majority of tested AML patient specimens showed sensitivity to the IBR + VEN combination, suggesting that the mechanism of efficacy of this combination is dramatically broader than a rare subset of AML. Importantly, while we observed that ex vivo sensitivity to IBR + VEN associated with higher levels of *BCL2* gene expression, we observed no significant association between IBR + VEN sensitivity and *BTK* expression. It remains possible that posttranslational modification of BTK could contribute to differences in sensitivity to IBR + VEN, though this finding may also be indicative of involvement of other ibrutinib targets in AML [15]. Beyond BTK, ibrutinib also potently inhibits several other kinases, including FLT3 and multiple TEC and SRC family members [32], which may provide therapeutic opportunities in other malignancies [43]. It is formally possible that ibrutinib acts on multiple targets in AML cells to achieve its enhanced sensitivity when combined with venetoclax. Notably, we identified increased expression in IBR + VEN sensitive samples for several ibrutinib targets (TEC, TXK, EGFR, and ERBB2) that contain a cysteine residue aligning with C481 in BTK, which is the covalent binding site for ibrutinib [32]. Each of these four kinases as well as FLT3 are reported to have in vitro IC_{50} values for ibrutinib below 100 nM [44], indicating that the effective concentrations of IBR + VEN could inhibit these targets and suggesting additional complexity with respect to ibrutinib sensitivity. With respect to FLT3, the association of FLT3-ITD mutations with sensitivity to ibrutinib has been established [15, 40, 41]. Moreover, elevated levels of TXK have been described in Behcet's disease, whose pathogenesis is associated with excessive Th1 cytokine production and inflammatory signaling [45].

Within the BCL2 family, higher expression levels of *BCL2A1* and *BCL2L11* (BIM) were detected in IBR + VEN resistant samples. This observation is consistent with prior studies that found that the elevated expression levels of *BCL2A1*, a BCR-regulated gene, are indicative of resistance to apoptosis inducers [46–48]. Many genes involved in cytokine signaling, including members of the IL-10 signaling pathway (as annotated by Reactome), were significantly upregulated in AML samples resistant to IBR + VEN, in a manner reminiscent of resistance mechanisms previously reported in MCLs [33]. Moreover, IL-6, an IL-10 signaling pathway member, has been shown to upregulate MCL1 and BCL-X_L in myeloma cells [49] or modulate MCL1:BIM priming [50], thereby promoting resistance to BCL2 family inhibitors. While these mechanisms may provide insight into IBR + VEN resistance, the majority of AML patient samples are sensitive to IBR + VEN, thus warranting consideration of this combination for AML therapy.

Acknowledgements Supported by grants from the National Cancer Institute (1U01CA217862, 1U54CA224019, 3P30CA069533). JWT received grants from the V Foundation for Cancer Research, the Gabrielle's Angel Foundation for Cancer Research, and the National Cancer Institute (1R01CA183947). AVD is a Leukemia and Lymphoma Society Scholar in Clinical Research. JWT has received research support from Agios, Aptose, Array, AstraZeneca, Constellation, Genentech, Gilead, Incyte, Janssen, Petra, Seattle Genetics, Syros, Takeda. BJD serves on the advisory boards for Gilead, Aptose, and Blueprint Medicines. BJD is principal investigator or coinvestigator on Novartis and BMS clinical trials. His institution, OHSU, has contracts with these companies to pay for patient costs, nurse and data manager salaries, and institutional overhead. He does not derive salary, nor does his laboratory receive funds from these contracts. The authors certify that the drugs tested in this study were chosen independently and without input from any of our industry partners. AVD received research support from Gilead Sciences, Genentech, Verastem Oncology, Bayer Oncology, Takeda Oncology, Bristol-Myers Squibb, MEI, Aptose Biosciences, AstraZeneca; honoraria and consulting fees from Abbvie, Pharmacyclics, Gilead Sciences, Verastem Oncology, TG Therapeutics, Celgene, Teva Oncology, AstraZeneca, Curis, Seattle Genetics, not relevant to this work.

Compliance with ethical standards

Conflict of interest This manuscript contains original research, has not been previously published, and is not under consideration for publication elsewhere. AVD has received commercial research grants from Gilead Sciences, Verastem, Takeda, AstraZeneca, and Verastem Oncology, and is a consultant/advisory board member for AbbVie, AstraZeneca, Genentech, Verastem Oncology, Seattle Genetics, TG Therapeutics, Curis, Celgene, Teva Oncology, and Gilead Sciences. BJD serves on the board of directors of Amgen, Burroughs Wellcome Fund, and CureOne; reports receiving other commercial research support from Novartis, Bristol-Myers Squibb, and Pfizer (institutional

funding—PI or coinvestigator on clinical trials funded via contract with OHSU); has ownership interest (including stock, patents, etc.) in Amgen, Blueprint Medicines, MolecularMD (inactive—acquired by ICON Laboratories), GRAIL, Patent 6958335 (exclusively licensed to Novartis), Henry Stewart Talks, Merck via Dana-Farber Cancer Institute (royalty payments); is a consultant/advisory board member for Aileron Therapeutics, ALLCRON, Third Coast Therapeutics, Monojul (inactive), Baxalta (inactive), CTI Biopharma (inactive), Aptose, Beta Cat, Blueprint Medicines, Celgene, Cepheid, GRAIL (former), Gilead (former), and Patient True Talk; and is an uncompensated joint steering committee member for Beat AML LLC. JWT has received commercial research grants from Agios, Aptose, Array, AstraZeneca, Constellation, Genentech, Gilead, Incyte, Janssen, Petra, Seattle Genetics, Syros, and Takeda; has received honoraria from the speakers bureaus of Therapeutic Advances in Childhood Leukemia and Hermedicus—Acute Leukemia Forum. No potential conflicts of interest were disclosed by the other authors.

References

1. Dohner H, Weisdorf DJ, Bloomfield CD. Acute myeloid leukemia. N Engl J Med. 2015;373:1136–52.
2. Medeiros BC, Satram-Hoang S, Hurst D, Hoang KQ, Momin F, Reyes C. Big data analysis of treatment patterns and outcomes among elderly acute myeloid leukemia patients in the United States. Ann Hematol. 2015;94:1127–38.
3. Konopleva M, Pollyea DA, Potluri J, Chyla B, Hogdal L, Busman T, et al. Efficacy and biological correlates of response in a phase II study of venetoclax monotherapy in patients with acute myelogenous leukemia. Cancer Discov. 2016;6:1106–17.
4. DiNardo CD, Pratz K, Pullarkat V, Jonas BA, Arellano M, Becker PS, et al. Venetoclax combined with decitabine or azacitidine in treatment-naive, elderly patients with acute myeloid leukemia. Blood. 2019;133:7–17.
5. Pollyea DA, Stevens BM, Jones CL, Winters A, Pei S, Minhajuddin M, et al. Venetoclax with azacitidine disrupts energy metabolism and targets leukemia stem cells in patients with acute myeloid leukemia. Nat Med. 2018;24:1859–66.
6. Hillmen P, Rawstron A, Brock K, Vicente SM, Yates F, Bishop R, et al. Ibrutinib plus venetoclax in relapsed/refractory CLL: results of teh bloodwise TAP clarity study. Blood. 2018;132:182.
7. Jain N, Keating MJ, Thompson PA, Ferrajoli A, Burger JA, Borthakur G, et al. Combined ibrutinib and venetoclax in patients with treatment-naive high-risk chronic lympocytic leukemia. Blood. 2018;132:696.
8. Rogers KA, Huang Y, Ruppert AS, Awan FT, Heerema NA, Hoffman C, et al. Phase 1b study of obinutuzumab, ibrutinib, and venetoclax in relapsed and refractory chronic lymphocytic leukemia. Blood. 2018;132:1568–72.
9. Tam CS, Anderson MA, Pott C, Agarwal R, Handunnetti S, Hicks RJ, et al. Ibrutinib plus venetoclax for the treatment of mantle-cell lymphoma. N Engl J Med. 2018;378:1211–23.
10. Byrd JC, Furman RR, Coutre SE, Flinn IW, Burger JA, Blum KA, et al. Targeting BTK with ibrutinib in relapsed chronic lymphocytic leukemia. N Engl J Med. 2013;369:32–42.
11. Chiron D, Dousset C, Brosseau C, Touzeau C, Maiga S, Moreau P, et al. Biological rational for sequential targeting of Bruton tyrosine kinase and Bcl-2 to overcome CD40-induced ABT-199 resistance in mantle cell lymphoma. Oncotarget. 2015;6:8750–9.
12. Cervantes-Gomez F, Lamothe B, Woyach JA, Wierda WG, Keating MJ, Balakrishnan K, et al. Pharmacological and protein profiling suggests venetoclax (ABT-199) as optimal partner with ibrutinib in chronic lymphocytic leukemia. Clin Cancer Res. 2015;21:3705–15.
13. Deng J, Isik E, Fernandes SM, Brown JR, Letai A, Davids MS. Bruton's tyrosine kinase inhibition increases BCL-2 dependence and enhances sensitivity to venetoclax in chronic lymphocytic leukemia. Leukemia. 2017;31:2075–84.
14. Friedman AA, Letai A, Fisher DE, Flaherty KT. Precision medicine for cancer with next-generation functional diagnostics. Nat Rev Cancer. 2015;15:747–56.
15. Tyner JW, Tognon CE, Bottomly D, Wilmot B, Kurtz SE, Savage SL, et al. Functional genomic landscape of acute myeloid leukaemia. Nature. 2018;562:526–31.
16. Tyner JW, Yang WF, Bankhead A 3rd, Fan G, Fletcher LB, Bryant J, et al. Kinase pathway dependence in primary human leukemias determined by rapid inhibitor screening. Cancer Res. 2013;73:285–96.
17. Altshuler B. Modeling of dose-response relationships. Environ Health Perspect. 1981;42:23–7.
18. Hansen KD, Irizarry RA, Wu Z. Removing technical variability in RNA-seq data using conditional quantile normalization. Biostatistics. 2012;13:204–16.
19. Love MI, Huber W, Anders S. Moderated estimation of fold change and dispersion for RNA-seq data with DESeq2. Genome Biol. 2014;15:550.
20. Leek JT, Storey JD. Capturing heterogeneity in gene expression studies by surrogate variable analysis. PLoS Genet. 2007;3:1724–35.
21. Buja A, Eyuboglu N. Remarks on parallel analysis. Multivar Behav Res. 1992;27:509–40.
22. Benjamini Y, Hochberg Y. Controlling the false discovery rate: a practical and powerful approach to multiple testing. J R Stat Soc Ser B Methodol. 1995;57:289–300.
23. Matthews L, Gopinath G, Gillespie M, Caudy M, Croft D, de Bono B, et al. Reactome knowledgebase of human biological pathways and processes. Nucleic Acids Res. 2009;37:D619–22.
24. Croft D, Mundo AF, Haw R, Milacic M, Weiser J, Wu G, et al. The Reactome pathway knowledgebase. Nucleic Acids Res. 2014;42:D472–7.
25. Sales G, Calura E, Cavalieri D, Romualdi C. graphite—a Bioconductor package to convert pathway topology to gene network. BMC Bioinforma. 2012;13:20.
26. Ibrahim MA, Jassim S, Cawthorne MA, Langlands K. A topology-based score for pathway enrichment. J Comput Biol. 2012;19:563–73.
27. Ihnatova I, Budinska E, Geistlinger L. ToPASeq: Topology-based pathway analysis of RNA-seq data. R package version 1.20.0. 2019.
28. Hochberg Y, A sharper Bonferroni procedure for multiple tests of significance. Biometrika. 1988;75:800.
29. Yadav B, Wennerberg K, Aittokallio T, Tang J. Searching for drug synergy in complex dose-response landscapes using an interaction potency model. Comput Struct Biotechnol J. 2015;13:504–13.
30. Zhang HW,B, Bottomly D, Kurtz SE, Eide CA, Damnernsawad A, Romine K, et al. Biomarkers predicting venetoclax sensitivity and strategies for venetoclax combination treatment. Blood. 2018;132:175.
31. Bisaillon R, Moison C, Thiollier C, Krosl J, Bordeleau ME, Lehnertz B, et al. Genetic characterization of ABT-199 sensitivity in human AML. Leukemia. 2020;34:63–74.
32. Pan Z, Scheerens H, Li SJ, Schultz BE, Sprengeler PA, Burrill LC, et al. Discovery of selective irreversible inhibitors for Bruton's tyrosine kinase. ChemMedChem. 2007;2:58–61.
33. Jayappa KD, Portell CA, Gordon VL, Capaldo BJ, Bekiranov S, Axelrod MJ, et al. Microenvironmental agonists generate de novo phenotypic resistance to combined ibrutinib plus venetoclax in CLL and MCL. Blood Adv. 2017;1:933–46.

34. Axelrod M, Ou Z, Brett LK, Zhang L, Lopez ER, Tamayo AT, et al. Combinatorial drug screening identifies synergistic co-targeting of Bruton's tyrosine kinase and the proteasome in mantle cell lymphoma. Leukemia. 2014;28:407–10.
35. Zhao X, Bodo J, Sun D, Durkin L, Lin J, Smith MR, et al. Combination of ibrutinib with ABT-199: synergistic effects on proliferation inhibition and apoptosis in mantle cell lymphoma cells through perturbation of BTK, AKT and BCL2 pathways. Br J Haematol. 2015;168:765–8.
36. Scheers E, Leclercq L, de Jong J, Bode N, Bockx M, Laenen A, et al. Absorption, metabolism, and excretion of oral (1)(4)C radiolabeled ibrutinib: an open-label, phase I, single-dose study in healthy men. Drug Metab Dispos. 2015;43:289–97.
37. Roberts AW, Davids MS, Pagel JM, Kahl BS, Puvvada SD, Gerecitano JF, et al. Targeting BCL2 with venetoclax in relapsed chronic lymphocytic leukemia. N Engl J Med. 2016;374:311–22.
38. DiNardo CD, Pratz K, Pullarkat V, Jonas BA, Arellano M, Becker PS, et al. Venetoclax combined with decitabine or azacitidine in treatment-naive, elderly patients with acute myeloid leukemia. Blood. 2019;133:7–17.
39. Lo-Coco F, Orlando SM, Platzbecker U. Treatment of acute promyelocytic leukemia. N Engl J Med. 2013;369:1472.
40. Rushworth SA, Murray MY, Zaitseva L, Bowles KM, MacEwan DJ. Identification of Bruton's tyrosine kinase as a therapeutic target in acute myeloid leukemia. Blood. 2014;123:1229–38.
41. Oellerich T, Mohr S, Corso J, Beck J, Dobele C, Braun H, et al. FLT3-ITD and TLR9 use Bruton tyrosine kinase to activate distinct transcriptional programs mediating AML cell survival and proliferation. Blood. 2015;125:1936–47.
42. Gutierrez A, Kentsis A. Acute myeloid/T-lymphoblastic leukaemia (AMTL): a distinct category of acute leukaemias with common pathogenesis in need of improved therapy. Br J Haematol. 2018;180:919–24.
43. Berglof A, Hamasy A, Meinke S, Palma M, Krstic A, Mansson R, et al. Targets for ibrutinib beyond B cell malignancies. Scand J Immunol. 2015;82:208–17.
44. Honigberg LA, Smith AM, Sirisawad M, Verner E, Loury D, Chang B, et al. The Bruton tyrosine kinase inhibitor PCI-32765 blocks B-cell activation and is efficacious in models of autoimmune disease and B-cell malignancy. Proc Natl Acad Sci USA. 2010;107:13075–80.
45. Suzuki N, Nara K, Suzuki T. Skewed Th1 responses caused by excessive expression of Txk, a member of the Tec family of tyrosine kinases, in patients with Behcet's disease. Clin Med Res. 2006;4:147–51.
46. Vogler M. BCL2A1: the underdog in the BCL2 family. Cell Death Differ. 2012;19:67–74.
47. Vogler M, Butterworth M, Majid A, Walewska RJ, Sun XM, Dyer MJ, et al. Concurrent up-regulation of BCL-XL and BCL2A1 induces approximately 1000-fold resistance to ABT-737 in chronic lymphocytic leukemia. Blood. 2009;113:4403–13.
48. Yecies D, Carlson NE, Deng J, Letai A. Acquired resistance to ABT-737 in lymphoma cells that up-regulate MCL-1 and BFL-1. Blood. 2010;115:3304–13.
49. Puthier D, Derenne S, Barille S, Moreau P, Harousseau JL, Bataille R, et al. Mcl-1 and Bcl-xL are co-regulated by IL-6 in human myeloma cells. Br J Haematol. 1999;107:392–5.
50. Gupta VA, Matulis SM, Conage-Pough JE, Nooka AK, Kaufman JL, Lonial S, et al. Bone marrow microenvironment-derived signals induce Mcl-1 dependence in multiple myeloma. Blood. 2017;129:1969–79.
51. He L, Kulesskiy E, Saarela J, Turunen L, Wennerberg K, Aittokallio T, et al. Methods for High-throughput Drug Combination Screening and Synergy Scoring. In: von Stechow L, editor. Cancer Systems Biology: Methods and Protocols. New York, NY: Springer New York. P351-398. 2018.